Weighted gene co-expression network analysis to identify key modules and hub genes associated with atrial fibrillation

WENYUAN LI[1], LIJUN WANG[1], YUE WU[1], ZUYI YUAN[1,2] and JUAN ZHOU[1,3]

[1]Department of Cardiovascular Medicine, The First Affiliated Hospital of Xi'an Jiaotong University;
[2]Key Laboratory of Environment and Genes Related to Diseases, Xi'an Jiaotong University, Ministry of Education;
[3]Key Laboratory of Molecular Cardiology of Shaanxi Province, Science and Technology Department of Shaanxi Province, Xi'an, Shaanxi 710061, P.R. China

Received April 12, 2019; Accepted November 8, 2019

DOI: 10.3892/ijmm.2019.4416

Abstract. Atrial fibrillation (AF) is the most common form of cardiac arrhythmia and significantly increases the risks of morbidity, mortality and health care expenditure; however, treatment for AF remains unsatisfactory due to the complicated and incompletely understood underlying mechanisms. In the present study, weighted gene co-expression network analysis (WGCNA) was conducted to identify key modules and hub genes to determine their potential associations with AF. WGCNA was performed in an AF dataset GSE79768 obtained from the Gene Expression Omnibus, which contained data from paired left and right atria in cardiac patients with persistent AF or sinus rhythm. Differentially expressed gene (DEG) analysis was used to supplement and validate the results of WGCNA. Gene Ontology and Kyoto Encyclopedia of Genes and Genomes enrichment analyses were also performed. Green and magenta modules were identified as the most critical modules associated with AF, from which 6 hub genes, acetyl-CoA Acetyltransferase 1, death domain-containing protein CRADD, gypsy retrotransposon integrase 1, FTX transcript, XIST regulator, transcription elongation factor A like 2 and minichromosome maintenance complex component 3 associated protein, were hypothesized to serve key roles in the pathophysiology of AF due to their increased intramodular connectivity. Functional enrichment analysis results demonstrated that the green module was associated with energy metabolism, and the magenta module may be associated with the Hippo pathway and contain multiple interactive pathways associated with apoptosis and inflammation. In addition, the blue module was identified to be an important regulatory module in AF with a higher specificity for the left atria, the genes of which were primarily correlated with complement, coagulation and extracellular matrix formation. These results suggest that may improve understanding of the underlying mechanisms of AF, and assist in identifying biomarkers and potential therapeutic targets for treating patients with AF.

Correspondence to: Professor Zuyi Yuan or Professor Juan Zhou, Department of Cardiovascular Medicine, The First Affiliated Hospital of Xi'an Jiaotong University, 277 West Yanta Road, Xi'an, Shaanxi 710061, P.R. China
E-mail: zuyiyuan@mail.xjtu.edu.cn
E-mail: 1306899042@qq.com

Key words: atrial fibrillation, weighted gene co-expression network analysis, hub genes, differentially expressed genes, atrial differences

Introduction

Atrial fibrillation (AF) is the most common form of cardiac arrhythmia and is a major contributor to morbidity, mortality and health care expenditure (1). Due to abnormal electrical activity and blood flow, AF is significantly associated with severe cardiac conditions, including stroke, heart failure and renal diseases (2). The mechanisms underlying AF are intricate and are typically classified as triggers or substrates, which result in electrophysiological remodeling and structural remodeling. Multiple molecular factors have been reported to be involved in pathophysiological progression, such as fibrosis, abnormal Ca^{2+} handling and inflammation (3-5). However, the exact mechanisms underlying the development and progression of AF are incompletely understood (3-5). In addition, unlike protein-coding genes, little is known about the long non-coding RNA (lncRNA) in AF; however, it has been demonstrated in a recent study that lncRNA may also serve an important role in AF by acting as competing endogenous RNAs (6). Although a number of therapies have been used to treat AF to prevent thrombotic events, cardioversion and control heart rhythm, the limited efficacy for cardioversion or correction of AF and the detrimental side effects of antiarrhythmic drugs or anticoagulants contribute to the challenge faced by clinicians when managing patients with AF (7). Therefore, there is an urgent requirement to elucidate the precise molecular mechanisms underlying AF, in order to identify appropriate therapeutic targets.

Recently, a number of algorithms and research methods have been developed to examine the potential mechanisms of gene networks, which provide comprehensive insights into specific diseases or conditions. Weighted gene co-expression network analysis (WGCNA) is one such tool, which divides gene co-expression networks of complex biological processes

into several characteristic modules (8). The modules are then used to analyze their association with clinical traits to find functional key modules (8). WGCNA has been used for analyzing a number of biological processes, including ontogeny (9), cancer (10-12) and mental disorders (13), and has been validated as a valuable method to identify underlying mechanisms, potential biomarkers or therapeutic targets in different types of diseases by placing a focus on key modules. Previous studies on the mechanisms of AF have primarily concentrated on specific pathophysiological functions, with relatively fewer studies identifying comprehensive regulatory networks. Therefore, in the present study, WGCNA was used to determine networks associated with AF.

The GSE79768 dataset was used in the present study, which contained 26 samples from paired left atria (LA) and right atria (RA) in patients with persistent AF or sinus rhythm (SR) (14). Two key modules with the highest level of significance correlation with AF were identified, and the 3 genes with the highest intramodular connectivity were selected as the hub genes in the respective modules for AF. As LA is more likely to serve as a driver of AF and AF-associated stroke than RA (15-17), the blue module was selected as a module of interest, as it was significantly correlated with both AF and LA, to further examine potential associations. Differentially expressed gene (DEG) analysis was additionally used, and the results were overlapped with WGCNA to further supplement and validate the results. The workflow used in the present study is presented in Fig. 1. The results may provide novel insight into the underlying mechanisms of AF and may assist the identification of potential biomarkers for diagnosis and treatment of AF.

Materials and methods

Dataset information. The AF dataset, GSE79768, was obtained from the NCBI Gene Expression Omnibus (GEO; https://www.ncbi.nlm.nih.gov/geo/). The dataset contains data from 13 pairs of left and right atrial appendages from 7 patients with persistent AF and 6 patients with SR (14). The dataset consisted of patients with AF whom presented with persistent AF for >6 months, or patients with SR with no evidence of AF and whom did not use any anti-arrhythmic drugs (14). The characteristics of the patients are summarized in Table SI, which may be downloaded from GEO (ncbi.nlm.nih.gov/geo/).

Microarray probe reannotation. Reannotation of microarray probes improves accuracy and makes it possible to identify new transcripts (18). Therefore, the probes of HG-U133_Plus_2.0 array in the dataset was reannotated based on a similar method used in previous studies (19,20). The probe sequences were downloaded from Affymetrix (affymetrix.com), and remapped to the human genome (GRCh38 release 94 primary assembly; ensembl.org/index.html) using the R package 'Rsubread' (http://www.bioconductor.org/packages/release/bioc/html/Rsubread.html) supported by the Bioconductor package (bioconductor.org/) (21). Uniquely mapped probes with no mismatches were retained. Subsequently, the chromosomal positions of these probes were matched to the corresponding genome annotation database in Ensembl using the R package 'GenomicRanges' (http://www.bioconductor.org/packages/release/bioc/html/GenomicRanges.html).

Probe sets that were mapped to >1 gene were removed to ensure the reliability of the reannotation. Following reannotation and removal of duplicated probes, 20,529 genes were retained, which included 16,285 protein coding genes and 3,243 lncRNAs according to the biotypes identified by Ensembl. As the non-coding genes may be associated with AF, WGCNA was performed on the top 5,000 genes from the reannotation results without partitions and other exclusions.

WGCNA. RAW data from the GSE79768 dataset were preprocessed and normalized using the R package 'affy' (http://www.bioconductor.org/packages/release/bioc/html/affy.html) and the 'rma' method. Subsequently, the genes were ranked by median absolute deviation from large to small, and the top 5,000 genes were selected for WGCNA using the R package 'WGCNA' (8,22). The power parameter ranging from 1-20 was screened out using the 'pickSoftThreshold' (package WGCNA) function. A suitable soft threshold of 5 was selected, as it met the degree of independence of 0.85 with the minimum power value. Subsequently, modules were constructed, and following dynamic branch cutting with a merging threshold of 0.25, 20 modules were obtained. The resulting gene network was visualized as a heatmap by randomly selecting 1,000 genes based on Topological Overlap Matrix dissimilarity and their cluster dendrogram.

Identification of key or modules of interest. Correlation between module eigengenes and clinical traits were analyzed to identify modules of interest that were significantly associated with clinical traits. The correlation values were displayed within a heatmap. Modules correlated with AF most significantly were considered as the key modules of AF. Gene significance (GS) was defined as the correlation between gene expression and each trait. In addition, module membership (MM) was defined as the association between gene expression and each module eigengene. Subsequently, the correlation between GS and MM were examined to verify certain module-trait associations. The correlation analyses in this study were performed using the Pearson correlation as described in the 'WGCNA' package (22).

Functional enrichment analysis of modules of interest. The genes in each module of interest were extracted from the network and enrichment analysis was performed to further explore the functions of the respective modules. The R package 'clusterProfiler' (23) (http://www.bioconductor.org/packages/release/bioc/html/clusterProfiler.html) was used to perform Gene Ontology (GO) (24,25) and Kyoto Encyclopedia of Genes and Genomes (KEGG) (26-28) pathway enrichment analysis. $P<0.05$ was set as the significance threshold, and the enrichment results of GO biological process (BP), GO molecular function (MF), GO cellular component (CC) and KEGG pathways in each module of interest module were obtained. Of the results that exceeded the threshold, the top 6 KEGG pathways and top 6 terms of each GO domain were identified.

Module visualization and identification of hub genes. The intramodular connectivity of genes in the corresponding modules of interest was measured using module eigengene

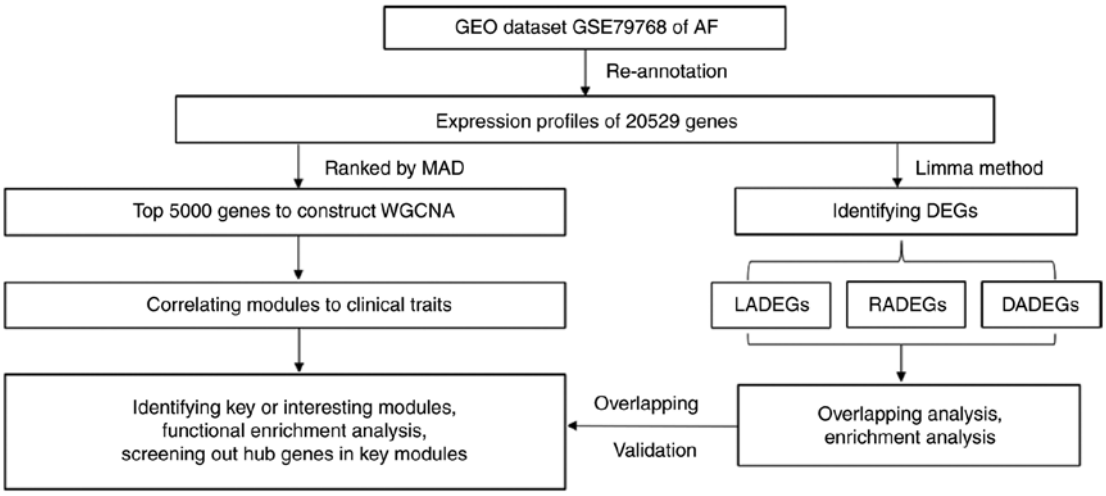

Figure 1. Flowchart of the bioinformatics methods used in the present study. GEO, Gene Expression Omnibus; AF, atrial fibrillation; MAD, median absolute deviation; WGCNA, weighted gene co-expression network analysis; DEGs, differentially expressed genes; LADEGs, differentially expressed genes in LA; RADEGs, differentially expressed genes in RA; DADEGs, differentially expressed genes in LA/RA ratio.

based connectivity kME. The top 30 genes of each modules of interest, which represented the central status in the module gene network, were selected to visualize the subordinate module using Cytoscape (v.3.7.0; cytoscape.org/) (29). Subsequently, two key modules were chosen which exhibited the highest levels of positive or negative correlation with AF to search for hub genes for AF in the modules. The top three genes with the highest kME were selected as the hub genes in the corresponding module (30) and their GS for AF and intramodular connectivity kME were determined to confirm the reliability of these hub genes.

DEG analysis and interactions with the modules of interest. The R package 'limma' was used to screen out DEGs among three sets of comparisons between AF and SR (31,32); left atria DEGs (LADEGs), right atria DEGs (RADEGs) and LA/RA ratio DEGs or DEGs of atrial differences (DADEGs). The cutoff for DEGs was a |fold change (FC)|>1.5 and P<0.05. The DEGs were visualized using the R package 'ggplot2' (https://cran.r-project.org/web/packages/ggplot2/) as a volcano plot (Fig. S1). Subsequently, the DEGs were overlapped with the modules of interest to identify potential links, the results of which are presented as a Venn diagram using the R package 'VennDiagram' (https://cran.r-project.org/web/packages/VennDiagram/). GO and KEGG enrichment analysis of upregulated or downregulated genes in each set of DEGs was performed, and their associations with the genes in the modules of interest were examined.

Validation of hub genes in public database. The expression profiles of hub genes in the key modules from the GSE79768 dataset were selected as representative genes used for validation. To verify these hub genes in an external dataset, GEO was searched with the key words 'atrial fibrillation'. The inclusion criteria for the validation dataset were as follows: i) Atria samples from individuals with persistent AF or SR; and ii) the sample size of each group was >5. Based on these criteria, 2 appropriate datasets were identified; GSE2240 and GSE115574. GSE2240 included data from 30 RA tissues obtained from 10 cardiac patients with persistent AF and 20 cardiac patients with SR. GSE115574 contained data from 14 LA tissues and 14 RA tissues from patients with AF and severe mitral regurgitation, and 15 LA tissues and 16 RA tissues from patients with AF and severe mitral regurgitation. Hub genes in the key modules were assessed for further validation. The expression profiles of these two microarray datasets were examined using the same methods as aforementioned for GSE79768.

Animal models. A total of 16 Sprague-Dawley male rats (body weight, 200-250g) were obtained from the Experimental Animal Center of Medical School, Xi'an Jiaotong University, and were kept in a specific-pathogen-free grade and temperature- and humidity-controlled facility on a 12:12 h light: Dark cycle with *ad libitum* access to food and water. This animal study was approved by the Institutional Ethics Committee for Animal Experiments of Xi'an Jiaotong University. All procedures conformed to the Guide for the Care and Use of Laboratory Animals published by the National Institutes of Health. Following acclimation under normal conditions for 1 week, the 16 rats were randomly assigned into 2 groups (control and AF). As described in a previous study (33), AF was induced by tail vein injection with acetylcholine (ACh) + $CaCl_2$ (60 μg/ml Ach; Sigma-Aldrich + 10 mg/ml $CaCl_2$; Beijing Solarbio Science & Technology Co., Ltd.) daily at 1 ml/kg for 1 week in the AF group (n=8). Rats in the control group (n=8) were injected with 0.9% normal saline daily via the tail vein at 1 ml/kg for 1 week. At baseline, all the rats were anesthetized with sodium pentobarbital [40 mg/kg; intraperitoneal (IP)]. Following anesthesia, the limb lead II electrocardiogram was recorded with limb leads inserted into the rat's limbs to ensure that all the rats had sinus rhythm at baseline. After 7 days of treatment, electrocardiogram test was performed on the rats again following anesthesia with sodium pentobarbital; 40 mg/kg IP). AF was induced successfully in all the rats in the AF group.

Reverse transcription-quantitative polymerase chain reaction (RT-qPCR) assay of atrial tissues. Total RNA was extracted

from both left atrial and right atrial tissues using TRIzol® Reagent (Thermo Fisher Scientific, Inc.) following the manufacturer's protocol. Purified RNA was reverse-transcribed into cDNA using PrimeScript™ RT Master Mix (Takara Bio, Inc.). Newly synthesized cDNA was analyzed by RT-qPCR using an iQ5 Multicolor Real-Time PCR detection system (Bio-Rad Laboratories, Inc.) with FastStart Essential DNA Green Master (Roche Diagnostics, Ltd.) according to the manufacturer's protocol. All the experiments were repeated in triplicate. The housekeeping gene β-actin was selected as the endogenous reference. The following primers were used in this study: β-actin forward, CTAAGGCCAACCGTG AAAAG; β-actin reverse, ACCAGAGGCATACAGGGACA; acetyl-CoA Acetyltransferase 1 (ACAT1) forward, GAGCAG AGGAGCAACACCATA; ACAT1 reverse, CTCAGCTTC TTCGCGGTGTT; death domain-containing protein CRADD (CRADD) forward, GTGGTACAGGTTCCCTATCAG; CRADD reverse, AGTGAGCGGAGAACTTGCTT; gypsy retrotransposon integrase 1 (GIN1) forward, ATCGTGGCT GCGGTTAGAG; GIN1 reverse, GCCATCCTTCCACCAGTT CTT; FTX transcript, XIST regulator (FTX) forward, CAG CAACACGCCAAGATGAA; FTX reverse, TGGGCAGGT TTGTGCGTAT; minichromosome maintenance complex component 3 associated protein (MCM3AP) forward, CTG GACCTGCCATCCTTTGT; and MCM3AP reverse, GCT GCCATCTCCTGTGAACT. The relative mRNA expression levels were then calculated using the $2^{-\Delta\Delta Cq}$ method (34).

Statistical analysis. Comparisons among groups were analyzed using analysis of variance followed by Tukey Honest Significant Differences post hoc test. The statistical analyses were performed in R v.3.5.1, and $P<0.05$ was considered to indicate a statistically significant difference.

Results

Construction of co-expression modules. The top 5,000 genes in 26 samples of paired left and right atrial appendages from 6 patients with SR and 7 patients with AF were used to construct the co-expression network. The results of cluster analysis of the samples are demonstrated in Fig. 2A. A soft-threshold power was introduced into the network topology, which affected the scale independence and mean connectivity of the network. Following screening, a soft-threshold of 5 was used to obtain the approximate scale-free topology with a scale-free topology fit index >0.85 and the lowest power (Fig. 2B). As indicated in Fig. 2C, 20 modules were identified, in which genes had similar co-expression traits. The size of these 20 modules are presented in Fig. 2D.

The interaction associations among these modules were analyzed. The network heatmap of a 1,000 randomly selected genes indicates a relatively high level of independence among these clusters (Fig. 3A). Furthermore, both the eigengene adjacency heatmap and the eigengene dendrogram indicated that these 20 modules could be divided into several smaller groups (Fig. 3B and C), suggesting that co-expression clusters with varying functions were present in the genetic networks of AF.

Correlation between modules and clinical traits. The module-trait associations were analyzed by correlating module-sample eigengenes with clinical traits to identify significant associations. The colors of all the modules were selected at random to distinguish between modules. Focusing on the status trait (AF and SR), the green module exhibited the highest positive correlation ($r=0.69$; $P<0.001$) and the magenta module ($r=-0.76$; $P<0.001$) exhibited the highest negative correlation (Fig. 3D). Therefore, these 2 modules were identified as key modules for AF. Additional associations were identified between MM and GS for specific traits. The significant correlations between green and magenta MM and GS for AF are presented in Fig. 4A and B. As previous studies demonstrated that differential left-to-right atria gene expression ratio may affect arrhythmogenesis and thrombogenesis of AF (14), which may suggest a specific co-expression pattern, the blue module was analyzed further as it exhibited a significant and relatively substantial correlation with both the LA ($r=0.53$; $P=0.006$) and AF ($r=-0.49$; $P=0.01$). Fig. 4C and D confirmed a significant association between the blue MM with GS for both AF and LA.

Functional enrichment analysis in modules of interest. GO and KEGG pathway enrichment analyses were performed on the green, magenta and blue gene clusters, and the top terms of each category are presented in Tables I and II. The KEGG pathway enrichment results demonstrated that the genes in the green module were primarily enriched in pathways associated with energy substance metabolism including amino acid metabolism, glycometabolism and lipid metabolism, in agreement with GO, BP and MF enrichment analysis. Results of GO CC analysis indicated that genes in the green module were primarily enriched in components associated with the mitochondria such as the mitochondrial membrane and matrix. Genes in the magenta module were enriched in several pathways primarily associated with apoptosis and inflammatory infiltration, including the Hippo signaling pathway, binding to receptor for advanced glycation end products receptor and positive regulation of NF-κB transcription factor activity. KEGG analysis indicated that the genes in the blue module were primarily enriched in complement and coagulation cascades. Furthermore, GO enrichment results demonstrated that blue module genes were significantly associated with complement activity and extracellular matrix (ECM) formation, such as complement activation, cell-cell adhesion mediator activity and ECM organization, which are all closely associated with coagulation, nonspecific immunity and cardiac remodeling.

Module visualization and identification of hub genes. The intramodular connectivity was ranked according to the kME value, and the top 30 genes of each module of interest was used to visualize the specific modules (Fig. 5). Subsequently, the top 3 genes of both the green and magenta modules were labeled as the hub genes for AF, as they were most positively or negatively statistically relevant modules with AF. The protein coding genes ACAT1, CRADD and GIN1 were selected as the hub genes in the green module for AF, and 1 lncRNA, FTX, and 2 protein coding genes, transcription elongation factor A like 2 (TCEAL2) and MCM3AP, were selected as the hub genes in the magenta module. All of these hub genes had a kME value >0.8 and relatively high GS for AF (>0.5; $P<0.01$), which established their network centrality and potential vital roles in AF.

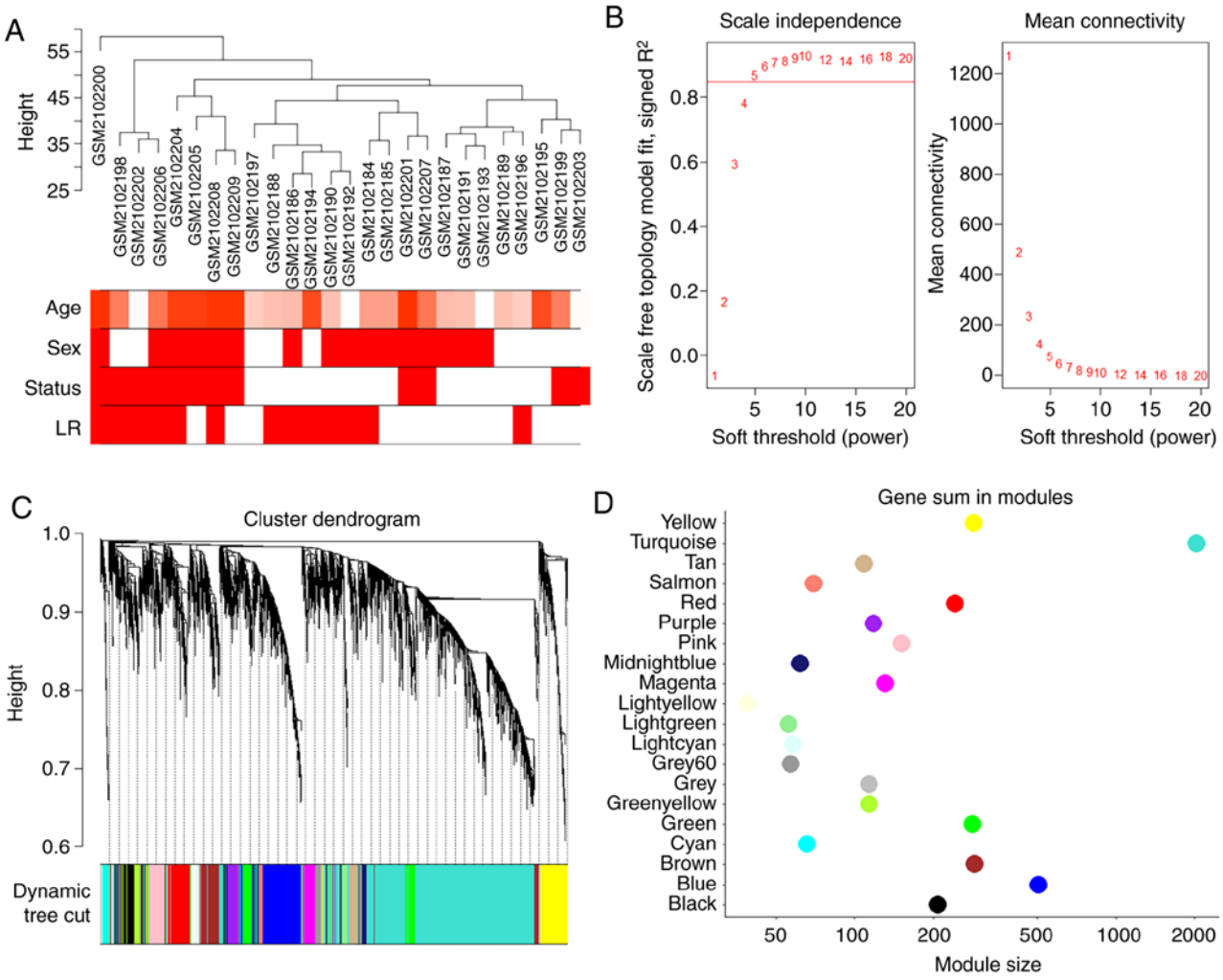

Figure 2. Construction of weighted co-expression network. (A) Sample dendrogram and trait heatmap. The colors represent the proportion to clinical traits including age, sex, status (AF and SR) and left atria or right atria. (B) Soft threshold selection process. (C) Cluster dendrogram. Each color represents one specific co-expression module, and branches above represent genes. (D) Module size. AF, atrial fibrillation; SR, sinus rhythm; MAD, median absolute deviation; WGCNA, weighted gene co-expression network analysis.

DEG analysis. DEG analysis was performed to validate the WGCNA results. Setting the cutoff as |FC|>1.5, with a P<0.05, 3 categories of DEG were screened between AF and SR in the LA, RA and the LA/RA ratio. A total of 497 upregulated (UP) LADEGs and 226 downregulated (DOWN) LADEGs, 104 UP RADEGs and 123 DOWN RADEGs and 203 DADEGs (133 UP and 70 DOWN) were identified. LADEGs had the highest number of DEGs among the 3 sets of comparisons; whereas RADEGs and DADEGs had similar sizes but considerably fewer DEGs. Volcano plots of these DEGs are presented in Fig. S1. The 3 different categories of DEGs were overlapped to additionally clarify their associations. As demonstrated in Fig. 6A, approximately two-thirds of the UP RADEGs and one-fourth of the DOWN RADEGs were also altered in LADEGs with a similar trend. The majority of DADEGs exhibited the same differential patterns as the LADEGs. These results (Fig. 6A and B) suggested that the sum of the UP and DOWN overlapping genes between LADEGs and RADEGs were identical with the total number of overlapping DEGs between LA (69 genes) and RA (32 genes), suggesting that few genes exhibited reversed expression when comparing LA to RA. Similarly, DADEGs exhibited a notable overlap with LADEGs but not with RADEGs, demonstrating that changes of the LA/RA ratio were primarily due to the overexpression or under-expression of LA genes. Enrichment analysis of these different kinds of DEGs are presented in Tables SII and SIII. The enrichment results demonstrated that LADEGs were significantly associated with a number of functions and pathways, including coagulation, inflammation and remodeling amongst others, suggesting a fairly complicated regulatory network in AF. Enrichment terms of RADEGs and DADEGs were both similar with LADEGs to a certain extent, which may explain their respective associations.

Association between DEGs and the modules of interest. Complex interactions and enrichment patterns of the aforementioned DEGs analysis highlighted the potential of integrated methods such as WGCNA to explore the gene co-expression network in AF. The green, magenta and blue modules were overlapped with the DEGs, in order to validate the results. The genes of both the green and magenta modules exhibited a degree of overlap with LADEGs or RADEGs, but almost no overlap with DADEGs (Fig. 6C and D). As these two modules were characteristically enriched in specific functions, some of

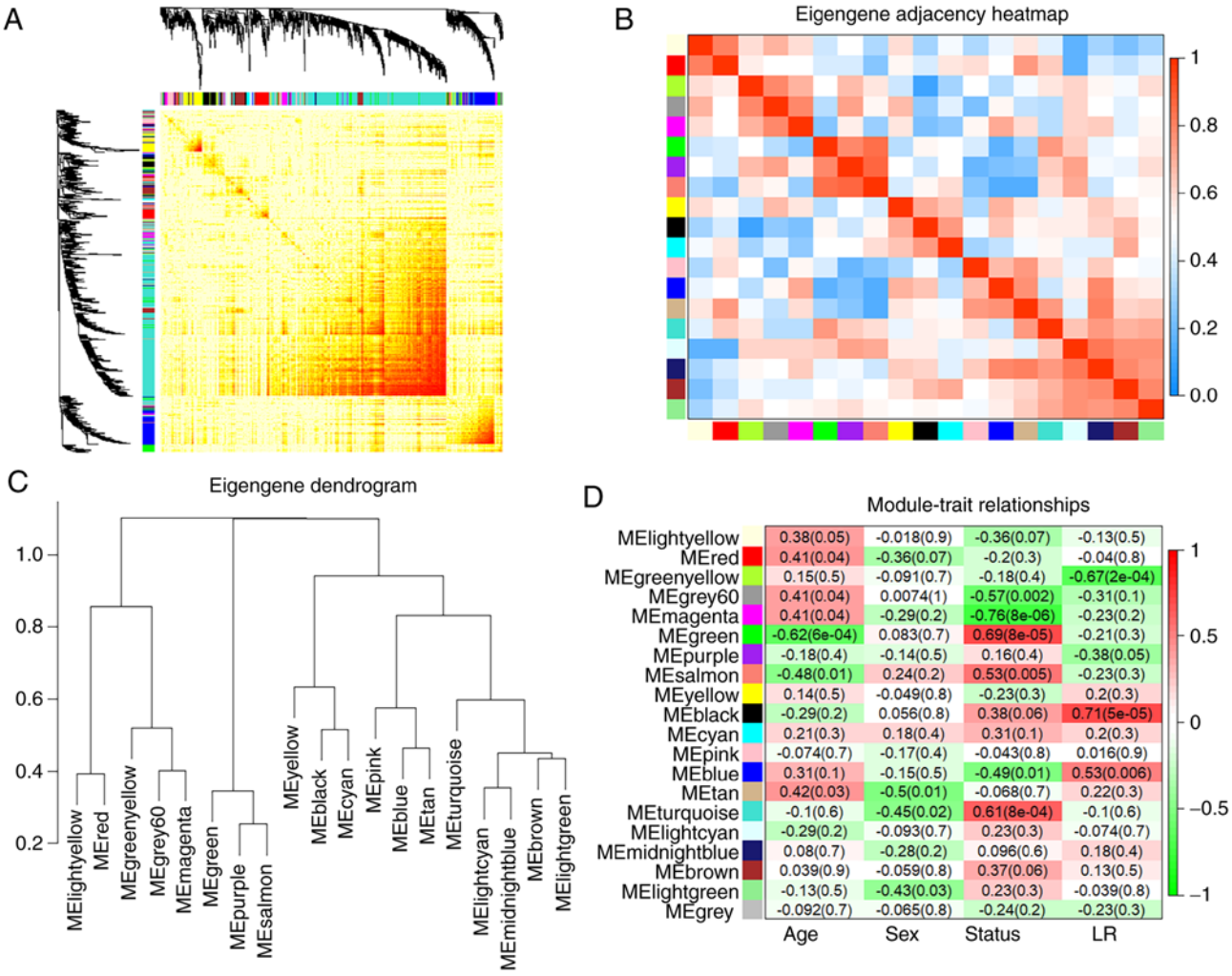

Figure 3. WGCNA module analysis. (A) Interaction of co-expression genes based on TOM dissimilarity and the cluster dendrogram of 1,000 randomly selected genes. The colors of the axes represent respective modules. The intensity of the yellow inside the heatmap represents the overlap degree of overlap, with a darker yellow representing an increased overlap. (B) Eigengene adjacency heatmap of different gene co-expression modules. (C) An eigengene dendrogram identified groups of correlated modules. (D) Heatmap of the correlation between clinical traits including age, sex, status (AF and SR), the left or right atria, and module eigengenes. Each column corresponds to a clinical trait, and each row corresponds to a module. Each cell contains the correlation coefficients which correspond to the cell color; green represents negative correlation and red represents positive correlation. The P-values are stated in the brackets. WGCNA, weighted gene co-expression network analysis; TOM, Topological Overlap Matrix; AF, atrial fibrillation; SR, sinus rhythm.

which were also parts of enriched pathways in the LADEGs or RADEGs, they may be used to validate the important functional roles of these two modules in AF. The genes of the blue module exhibited the largest amount of overlap with the downregulated genes of LADEGs and DADEGs, confirming the association between the blue module with AF and LA. Genes in the blue module also showed notably less overlap with the RADEGs (Fig. 6E and F), similar to the overlapping patterns of DADEGs. Enrichment results also demonstrated that several significant pathways associated with the blue module were similar to pathways associated with the down-regulated DADEGs or LADEGs. Overall, the comparisons between DEGs and modules of interest verified the reliability of the WGCNA.

Validation of hub genes in public database. Although none of the green module hub genes were present in the clusters of LADEGs, RADEGs or DADEGs, they were all significantly overexpressed in the LA or RA in AF compared with SR. However, no statistical difference in the LA/RA ratios was observed between the AF and SR groups (Fig. 7A-C). Similarly, only 1 magenta hub gene, TCEAL2, was present in the LADEGs and RADEGs; FTX was present in the LADEGs and MCM3AP was not present in either. Nevertheless, the expression levels of all 3 genes were significantly down-regulated in both LA and RA, and were not differentially expressed in LA/RA ratio (Fig. 7D-F). These results demonstrated the validity of the hub genes identified the in green and magenta modules. Through further validation of the hub genes in other datasets (Table SIV), it was identified that CRADD was significantly upregulated in AF compared with SR in the RA in GSE115574. The expression levels of ACAT1 and FTX in the RA in GSE115574 were in agreement with the results of analysis of the GSE79768 dataset (ACAT1, P=0.06; FTX, P=0.05). FTX and TCEAL2 expression was also significantly decreased in AF in the GSE2240 dataset. As the datasets varied in sample size and had different criteria for inclusion/exclusion, not all of the hub genes identified in the GSE79768 dataset

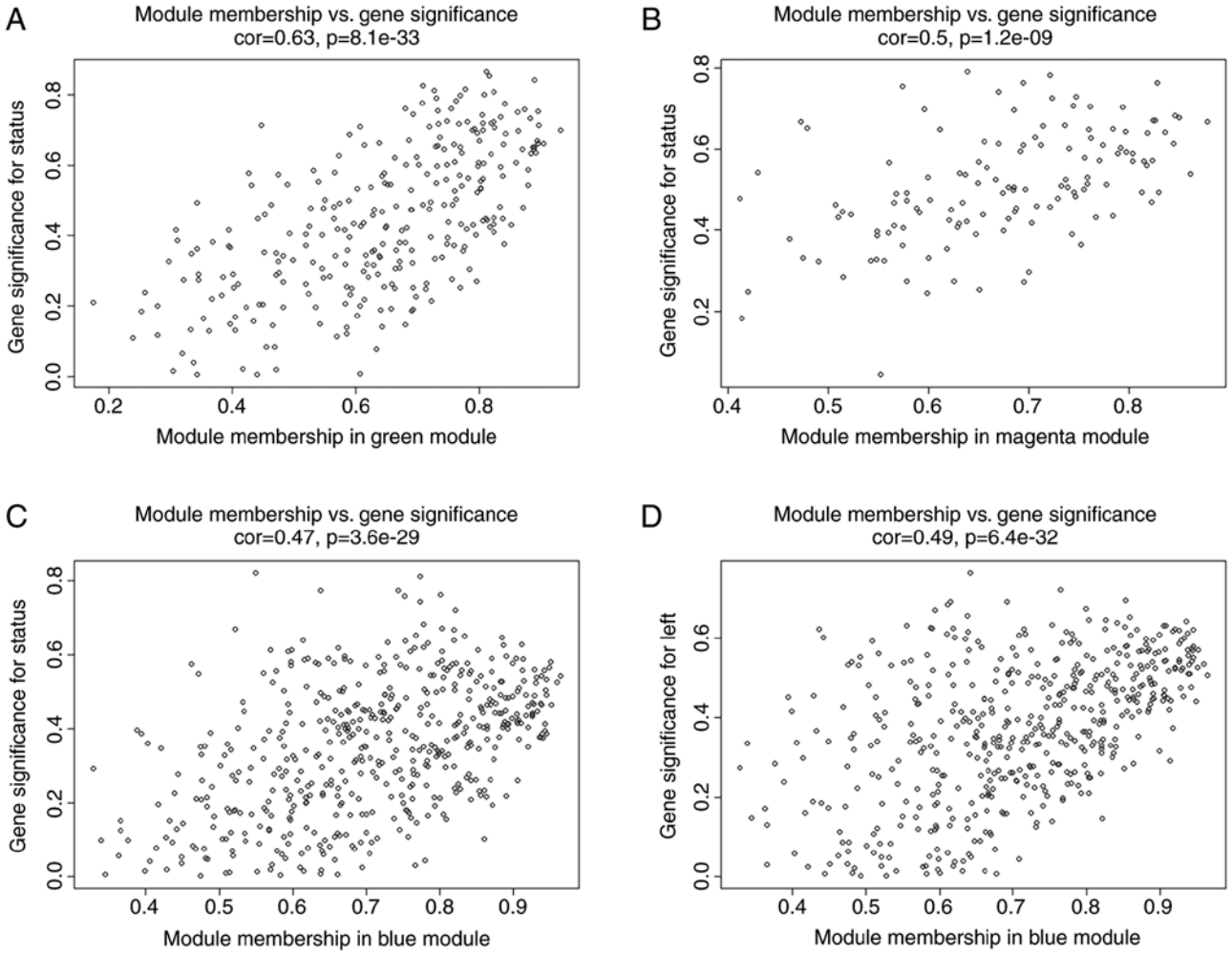

Figure 4. Correlation between MM of modules of interest and GS with clinical traits. (A) Scatter plot of GS for AF vs. MM in the green module. (B) Scatter plot of GS for AF vs. MM in the magenta module. (C) Scatterplot of GS for AF vs. MM in the blue module. (D) Scatter plot of GS for LA vs. MM in the blue module. GS, gene significance; AF, atrial fibrillation; MM, module membership; LA, left atria.

were verified in the other two datasets. In addition, as patients had different cardiovascular diseases between the datasets, the potential differences in the comorbidities and demographics of the patients may represent confounding variables. As such, additional studies and datasets are required to verify the value of these hub genes.

Validation of hub genes in AF rat models. As TCEAL2 is not present in the rat genome, the expression levels of the other 5 hub genes were measured for validation in the AF rat model generated in the present study. As demonstrated in Fig. 8B-D, the expression levels of hub genes ACAT1, CRADD and GIN1 in RA were all significantly increased in AF group compared with those in control (SR) group ($P<0.05$). In LA, the expression level of GIN1 was significantly increased in the AF group ($P<0.001$; Fig. 8D), and the expression levels of lncRNA FTX was significantly decreased compared with those in control group ($P<0.05$; Fig. 8E). Besides, the expression levels of ACAT1 and CRADD in LA were observed to be increased in AF group, and the expression levels of FTX in RA were decreased in AF group, but these differences were not statistically significant. In addition, there was no significant difference in the LA/RA ratios between the AF and control groups in any of these hub genes. These results were in concordance with the results of the primary dataset (Fig. 7). However, no statistically significant expression difference in MCM3AP was identified between the AF and control groups in either the LA or RA.

Discussion

AF is the most common type of cardiac arrhythmia and is associated with a poor prognosis in patients with cardiac diseases (1); however, treatments for patients with AF remain unsatisfactory (35). The underlying pathophysiological mechanisms of AF are extremely complicated, thus WGCNA may be an effective method of mining valuable data to analyze complicated genetic networks. In the present study, WGCNA was performed using R with an AF dataset, which contained gene expression data from paired left and right atrial tissues from cardiac patients with AF or SR. The green and magenta modules were identified as the key modules of AF, with the highest level of significant associations with AF. The top 3 genes of each key module with the highest intramodular connectivity were identified as hub genes for AF. In addition, another module of interest was selected that was associated with both AF and LA, to examine the potential association

Table I. KEGG enrichment analysis in interesting modules.

Module	ID	Description	P-value	Count
Green	hsa00280	Valine, leucine and isoleucine degradation	0.00013	5
Green	hsa00250	Alanine, aspartate and glutamate metabolism	0.003972	3
Green	hsa01200	Carbon metabolism	0.00591	5
Green	hsa03420	Nucleotide excision repair	0.008537	3
Green	hsa00071	Fatty acid degradation	0.009175	3
Green	hsa01212	Fatty acid metabolism	0.013585	3
Magenta	hsa04390	Hippo signaling pathway	0.000993	5
Magenta	hsa04060	Cytokine-cytokine receptor interaction	0.01245	5
Magenta	hsa04550	Signaling pathways regulating pluripotency of stem cells	0.033364	3
Magenta	hsa00590	Arachidonic acid metabolism	0.034535	2
Magenta	hsa05224	Breast cancer	0.039373	3
Magenta	hsa05226	Gastric cancer	0.040072	3
Blue	hsa04610	Complement and coagulation cascades	6.51×10^{-7}	12
Blue	hsa05133	Pertussis	0.000178	9
Blue	hsa04976	Bile secretion	0.003199	7
Blue	hsa05222	Small cell lung cancer	0.005002	8
Blue	hsa05150	Staphylococcus aureus infection	0.009243	5
Blue	hsa04530	Tight junction	0.017169	10

KEGG, Kyoto Encyclopedia of Genes and Genomes.

between AF and the genetic differences between the LA and RA. The results of the enrichment analysis suggested that the modules of interest used in the present study were associated with the pathological processes of energy metabolism, inflammation and apoptosis, coagulation, complement or ECM formation. These results provided a partial description of the comprehensive regulatory network in AF, which may improve the current understanding of the mechanisms underlying AF, and may assist in identifying potential therapeutic targets.

The present study used the GEO dataset GSE79768 to perform WGCNA. The original study involving this dataset, conducted by Tsai *et al* (14), revealed the differences between LA-to-RA transcriptional profiles between AF and SR, and suggested that AF was associated with differential LA-to-RA gene expression, which was related to specific ion channels and pathways, as well as upregulation of thrombogenesis-associated genes in the LA appendage. The major differences in the genes or modules obtained in the present study, compared with the results from the study by Tsai *et al* (14) was that the present study used a more comprehensive method, WGCNA, not only identifying the blue module as an important regulatory module of AF with increased specificity in the LA associated with complement, coagulation and extracellular matrix formation, expanding upon their results in LA-to-RA DEGs associated-pathways, but also identifying 2 critical modules for AF: The green module, which was associated with energy metabolism; and the magenta module, which was associated with multiple interactive pathways associated with apoptosis and inflammation. The in-depth analyses performed in the present and the results obtained cannot be obtained from conventional microarray DEGs analyses.

Among the 20 modules identified by WGCNA, the green module exhibited the greatest positive correlation with AF. Enrichment analysis indicated that the genes in the green module were primarily associated with pathways related to energy substance metabolism and potentially located in the mitochondria. Several studies have suggested that altered atrial metabolism may serve an important role in the pathophysiology of AF (36-38). Previous genomic, metabolomic and proteomic studies have also demonstrated that metabolic genes and products were notably altered in patients with AF compared to patients with SR (39,40). As a result of irregular high-frequency excitation and contraction, AF-associated metabolic stress occurs when there is a decreased capacity of energy to supplement the demands of atrial tissues, combined with an increase in metabolism of ketone bodies, AMPK activation, mitochondria dysfunction and reactive oxygen species generation, which accelerates gradual atrial remodeling (41). KEGG pathway analysis of the magenta module indicated that it was primarily associated with the Hippo signaling pathway. The Hippo pathway is a highly conserved mammalian pathway, involved in regulation of cell proliferation, apoptosis and other cellular functions, and serves an important role in the development of the heart, regeneration and cardiac diseases (42-44). Although, to the best of our knowledge, there are currently no studies investigating the role of the Hippo pathway in AF, several recent studies have demonstrated its role in myocardial infarction, hypertrophy and heart failure (43). Del Re *et al* (45) revealed that depletion of Yes-associated protein isoform 1 (Yap1), a downstream protein in the Hippo pathway, augmented apoptosis and fibrosis and decreased compensatory cardiomyocyte hypertrophy, thereby exacerbating injury following chronic myocardial infarction, suggesting that Yap1

Table II. GO enrichment analysis in interesting modules.

Module	Category	ID	Description	P-value	Count
Green	BP	GO:0006520	Cellular amino acid metabolic process	$4.71x10^{-5}$	14
Green	BP	GO:0009083	Branched-chain amino acid catabolic process	0.0001	4
Green	BP	GO:1901605	Alpha-amino acid metabolic process	0.000106	11
Green	BP	GO:0009063	Cellular amino acid catabolic process	0.000125	8
Green	BP	GO:0009081	Branched-chain amino acid metabolic process	0.00019	4
Green	BP	GO:1901606	Alpha-amino acid catabolic process	0.000258	7
Green	MF	GO:0016790	Thiolester hydrolase activity	0.000692	4
Green	MF	GO:0005496	Steroid binding	0.000985	6
Green	MF	GO:0016289	CoA hydrolase activity	0.001351	3
Green	MF	GO:0015485	Cholesterol binding	0.002827	4
Green	MF	GO:0032934	Sterol binding	0.004602	4
Green	MF	GO:0048037	Cofactor binding	0.009342	13
Green	CC	GO:0005743	Mitochondrial inner membrane	$4.77x10^{-7}$	20
Green	CC	GO:0044455	Mitochondrial membrane part	$2.56x10^{-6}$	13
Green	CC	GO:0019866	Organelle inner membrane	$3.83x10^{-6}$	20
Green	CC	GO:0005759	Mitochondrial matrix	$1.42x10^{-5}$	18
Green	CC	GO:0098800	Inner mitochondrial membrane protein complex	$2.25x10^{-5}$	9
Green	CC	GO:0098798	Mitochondrial protein complex	$5.73x10^{-5}$	12
Magenta	BP	GO:0051091	Positive regulation of DNA binding transcription factor activity	0.000163	8
Magenta	BP	GO:0051092	Positive regulation of NF-kappaB transcription factor activity	0.000236	6
Magenta	BP	GO:0030901	Midbrain development	0.000261	5
Magenta	BP	GO:0061564	Axon development	0.000312	11
Magenta	BP	GO:0030593	Neutrophil chemotaxis	0.000397	5
Magenta	BP	GO:1990266	Neutrophil migration	0.000662	5
Magenta	MF	GO:0050786	RAGE receptor binding	$4.83x10^{-7}$	4
Magenta	MF	GO:0005504	Fatty acid binding	0.00122	3
Magenta	MF	GO:0017147	Wnt-protein binding	0.002081	3
Magenta	MF	GO:0035325	Toll-like receptor binding	0.002156	2
Magenta	MF	GO:0036041	Long-chain fatty acid binding	0.003685	2
Magenta	MF	GO:0004115	3',5'-cyclic-AMP phosphodiesterase activity	0.004916	2
Magenta	CC	GO:0030017	Sarcomere	0.007341	5
Magenta	CC	GO:0044449	Contractile fiber part	0.010578	5
Magenta	CC	GO:0030016	Myofibril	0.010794	5
Magenta	CC	GO:0043025	Neuronal cell body	0.011374	8
Magenta	CC	GO:0034774	Secretory granule lumen	0.01299	6
Magenta	CC	GO:0043292	Contractile fiber	0.013378	5
Blue	BP	GO:0006958	Complement activation, classical pathway	$1.45x10^{-8}$	10
Blue	BP	GO:0030198	Extracellular matrix organization	$9.86x10^{-8}$	30
Blue	BP	GO:0043062	Extracellular structure organization	$2.34x10^{-7}$	32
Blue	BP	GO:0002455	Humoral immune response mediated by circulating immunoglobulin	$3.57x10^{-7}$	10
Blue	BP	GO:0006956	Complement activation	$1.54x10^{-6}$	11
Blue	BP	GO:0030449	Regulation of complement activation	$2.89x10^{-6}$	9
Blue	MF	GO:0098632	Cell-cell adhesion mediator activity	$7.45x10^{-5}$	8
Blue	MF	GO:0017171	Serine hydrolase activity	$8.63x10^{-5}$	16
Blue	MF	GO:0004714	Transmembrane receptor protein tyrosine kinase activity	$9.32x10^{-5}$	9
Blue	MF	GO:0005201	Extracellular matrix structural constituent	0.00013	14
Blue	MF	GO:0008236	Serine-type peptidase activity	0.000227	15
Blue	MF	GO:0098631	Cell adhesion mediator activity	0.000228	8
Blue	CC	GO:0031012	Extracellular matrix	$4.57x10^{-5}$	35
Blue	CC	GO:0016324	Apical plasma membrane	$1.66x10^{-5}$	23
Blue	CC	GO:0062023	Collagen-containing extracellular matrix	$2.44x10^{-5}$	24
Blue	CC	GO:0005604	Basement membrane	$5.91x10^{-5}$	11

Table II. Continued.

Module	Category	ID	Description	P-value	Count
Blue	CC	GO:0005911	Cell-cell junction	0.000122	27
Blue	CC	GO:0045177	Apical part of cell	0.000132	24

GO, Gene Ontology; BP, biological process; MF, molecular function; CC, cellular component.

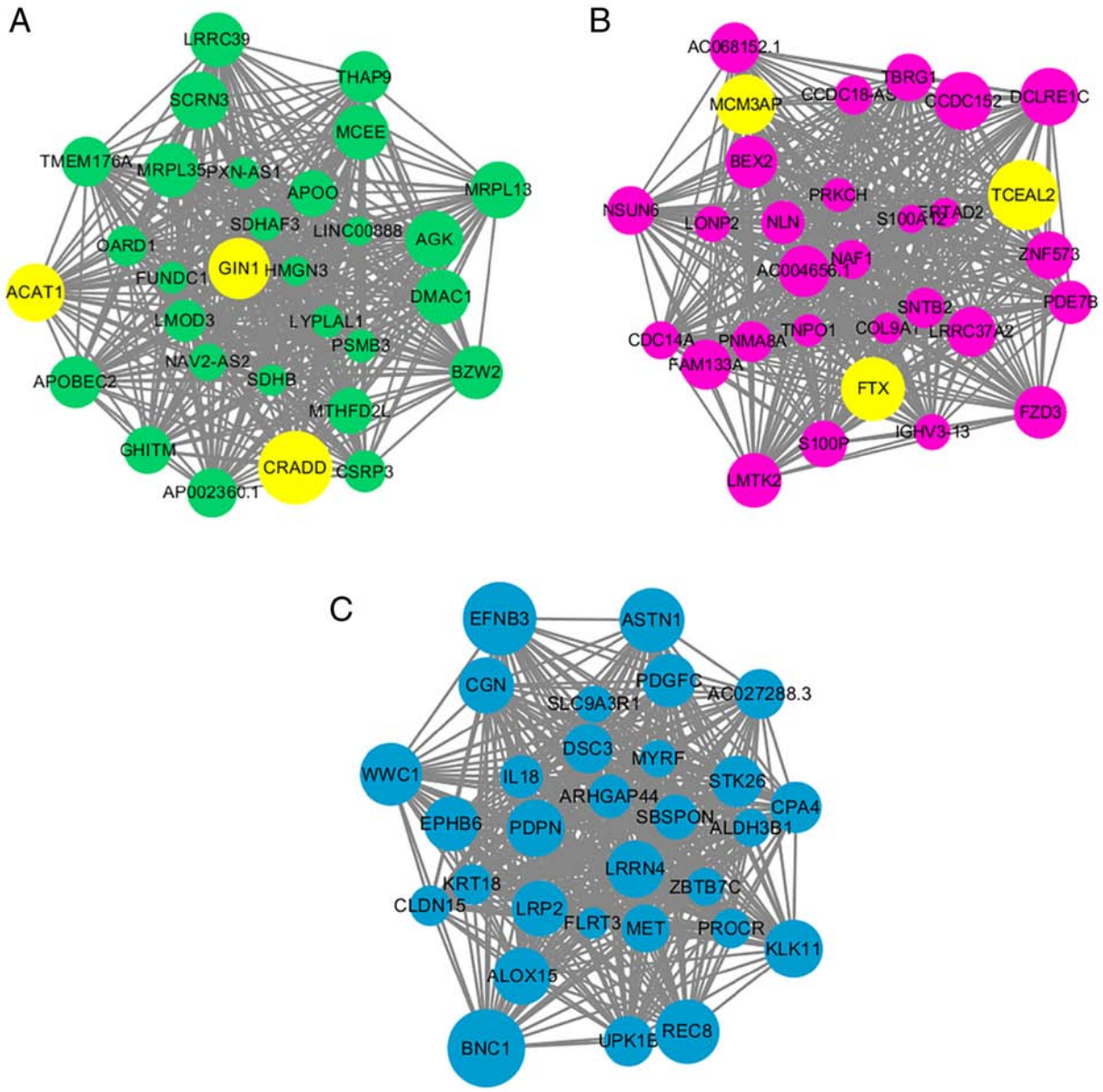

Figure 5. Visualization of modules of interest and hub genes. (A) The top 30 genes with the highest levels of intramodular connectivity in the green module. Genes highlighted yellow are the top 3 hub genes. The size of the circle is proportional to the intramodular connectivity. (B) The top 30 genes in magenta module. Genes highlighted yellow are the hub genes. (C) The top 30 genes in the blue module.

is critical in the homeostasis of the physiological processes of the heart. Leach *et al* (46) demonstrated that deletion of the Hippo pathway component Salvador (Salv) in mouse hearts with ischemic heart failure following myocardial infarction decreased fibrosis, increased scar border vascularity and recovery of the pumping function, thus reversing heart failure; whereas the Yap target gene Parkin RBR E3 ubiquitin protein ligase was essential for heart repair in Salv knock-out mice. The Hippo pathway interacts with multiple transcription factors that affects a variety of genes and pathways including proinflammatory genes and the Wnt pathway (43,44), and these interactions were also predicted by GO enrichment

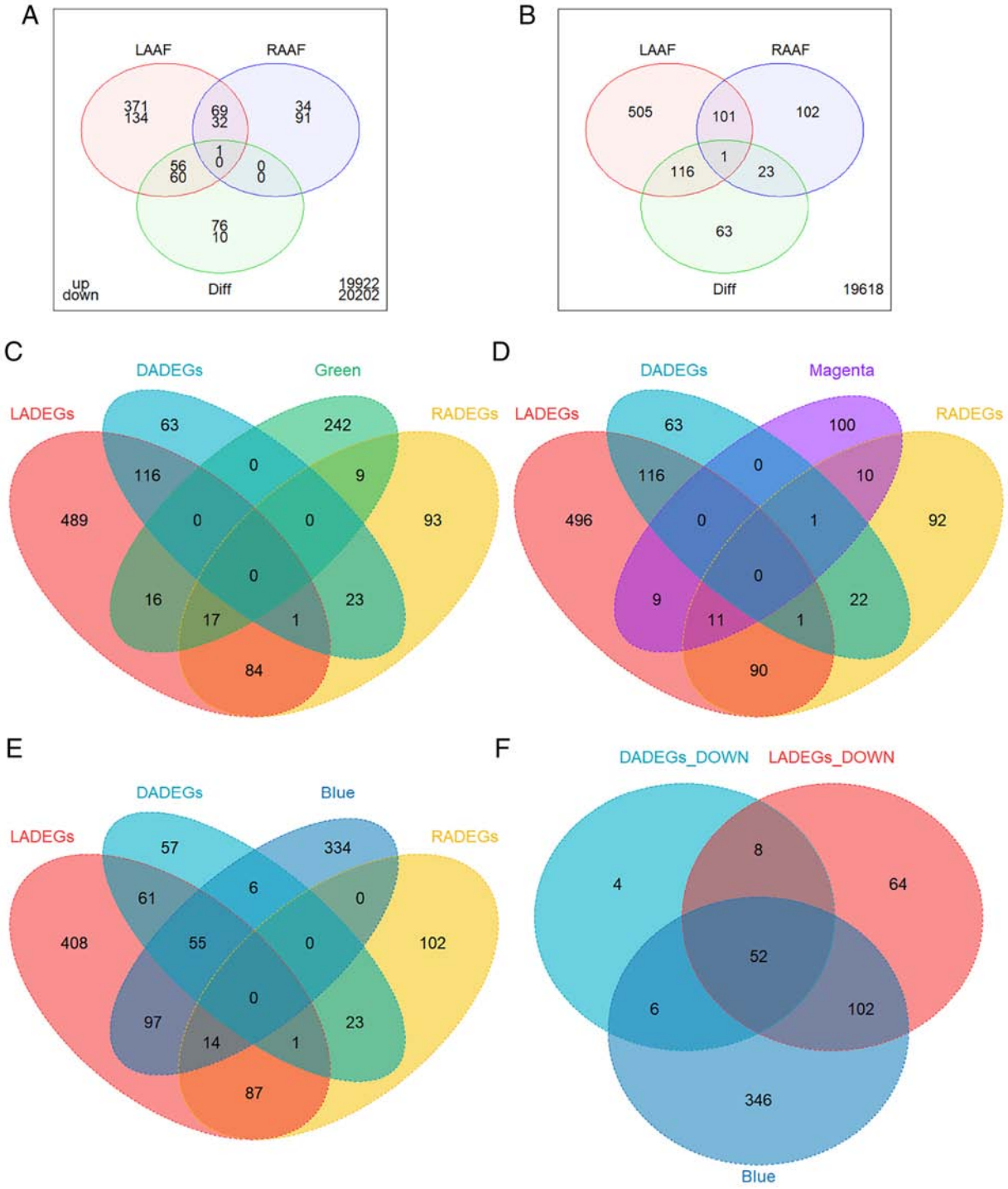

Figure 6. Overlap of DEGs and modules of interest. (A) Venn diagram of LADEGs, RADEGs and DADEGs in UP DEGs (above) and DOWN DEGs (below). The numbers outside the diagram represent the sum of genes which did not belong to any category of DEG. Venn diagram of LADEGs, RADEGs and DADEGs and the (B) total DEGs, (C) genes of the green module, (D) genes of the magenta module, and (E) genes of the blue module. (F) Venn diagram of DOWN LADEGs, DOWN DADEGs and genes of the blue module. DEGs, differentially expressed genes; LA, left atria; RA, right atria; LADEGs, differentially expressed genes in the LA; RA, right atria; RADEGs, differentially expressed genes in the RA; DADEGs, differentially expressed genes in LA/RA ratio; UP, upregulated; DOWN, downregulated.

of the magenta module in the present study. Furthermore, apoptosis and fibrotic activation mediated by inflammation may contribute to structural remodeling of the atria (35), and the Hippo pathway is involved in these pathological mechanisms in cardiovascular systems (43). Therefore, the magenta module may be an integrated functional cluster that regulates myocardial apoptosis, inflammation and remodeling, and may be mediated by the Hippo pathway. Further exploration of this module is required to identify the precise mechanisms associated with the development of AF.

As the green and magenta modules exhibited the highest levels of positive and negative correlation with AF, the hub genes in these modules were screened. The top 3 genes in each module were identified as the intramodular hub genes of AF

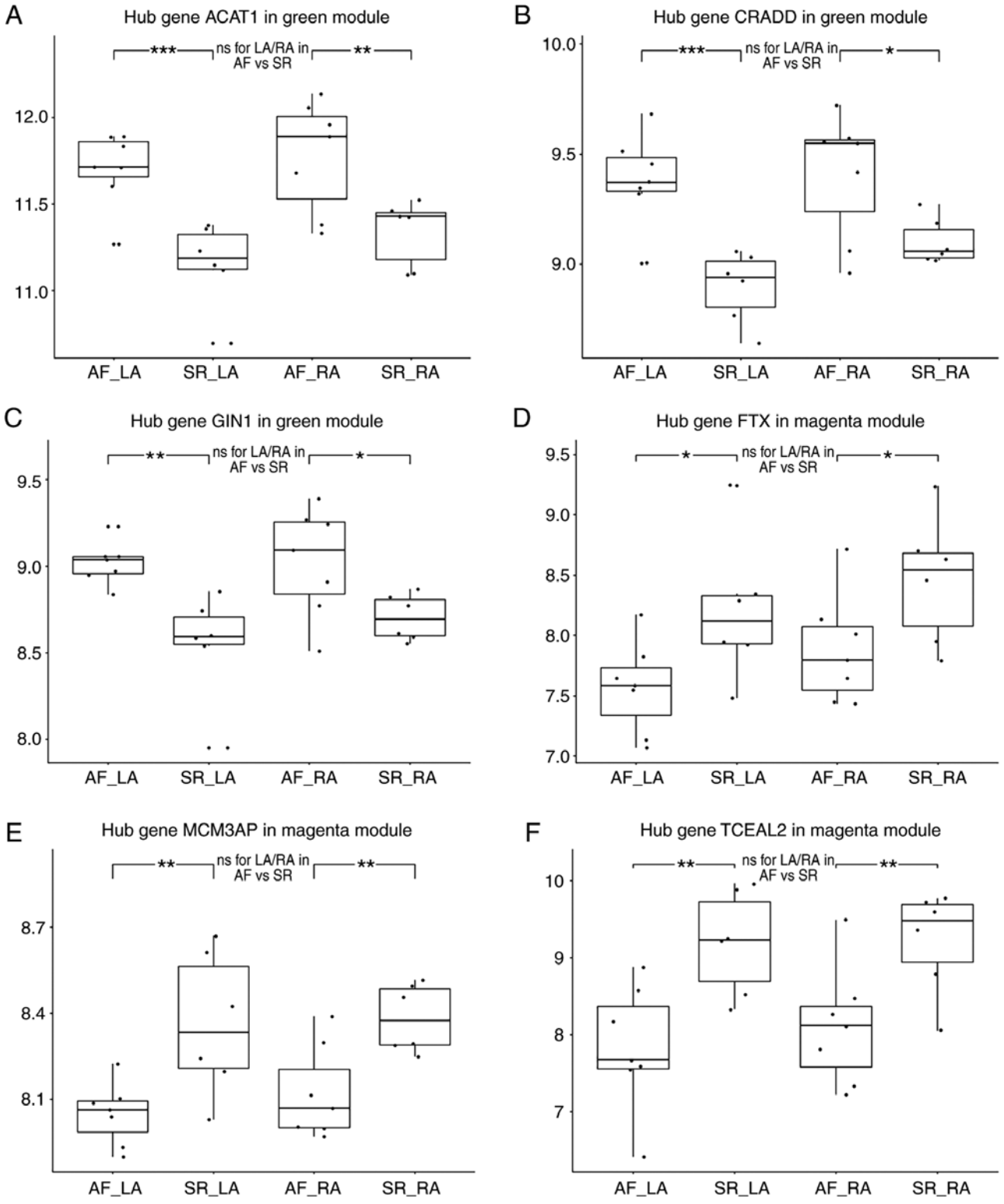

Figure 7. Validation of hub genes at the expressional level. Validation of hub genes (A) ACAT1, (B) CRADD and (C) GIN1 in the green module. Expression values of each hub gene in the LA of AF, LA of SR, RA of AF, RA of SR, from left to right. These hub genes were significantly overexpressed in both LA and RA compared with SR, while no statistical difference was observed the in LA/RA ratio. Validation of the hub genes (D) FTX, (E) MCM3AP and (F) TCEAL2 in the magenta module. These hub genes were downregulated, and no statistically significant difference was observed in the LA/RA ratio. AF, atrial fibrillation; LA, left atria; SR, sinus rhythm; RA, right atria; ns, no statistical difference; *P<0.05, **P<0.01 and ***P<0.001. ACAT1, acetyl-CoA Acetyltransferase 1; CRADD, death domain-containing protein CRADD; GIN1, gypsy retrotransposon integrase 1; LA, left atria; AF, atrial fibrillation; SR, sinus rhythm; RA, right atria; FTX, FTX transcript, XIST regulator; MCM3AP, minichromosome maintenance complex component 3 associated protein; TCEAL2, transcription elongation factor A like 2.

following confirmation of their close association with AF. A total of 3 protein coding genes, ACAT1, CRADD and GIN1 in the green module, and 1 lncRNA, FTX, and 2 protein coding genes TCEAL2 and MCM3AP in the magenta module were identified. ACAT1 is expressed in macrophages, and it has been demonstrated that it generates cholesterol ester of foam

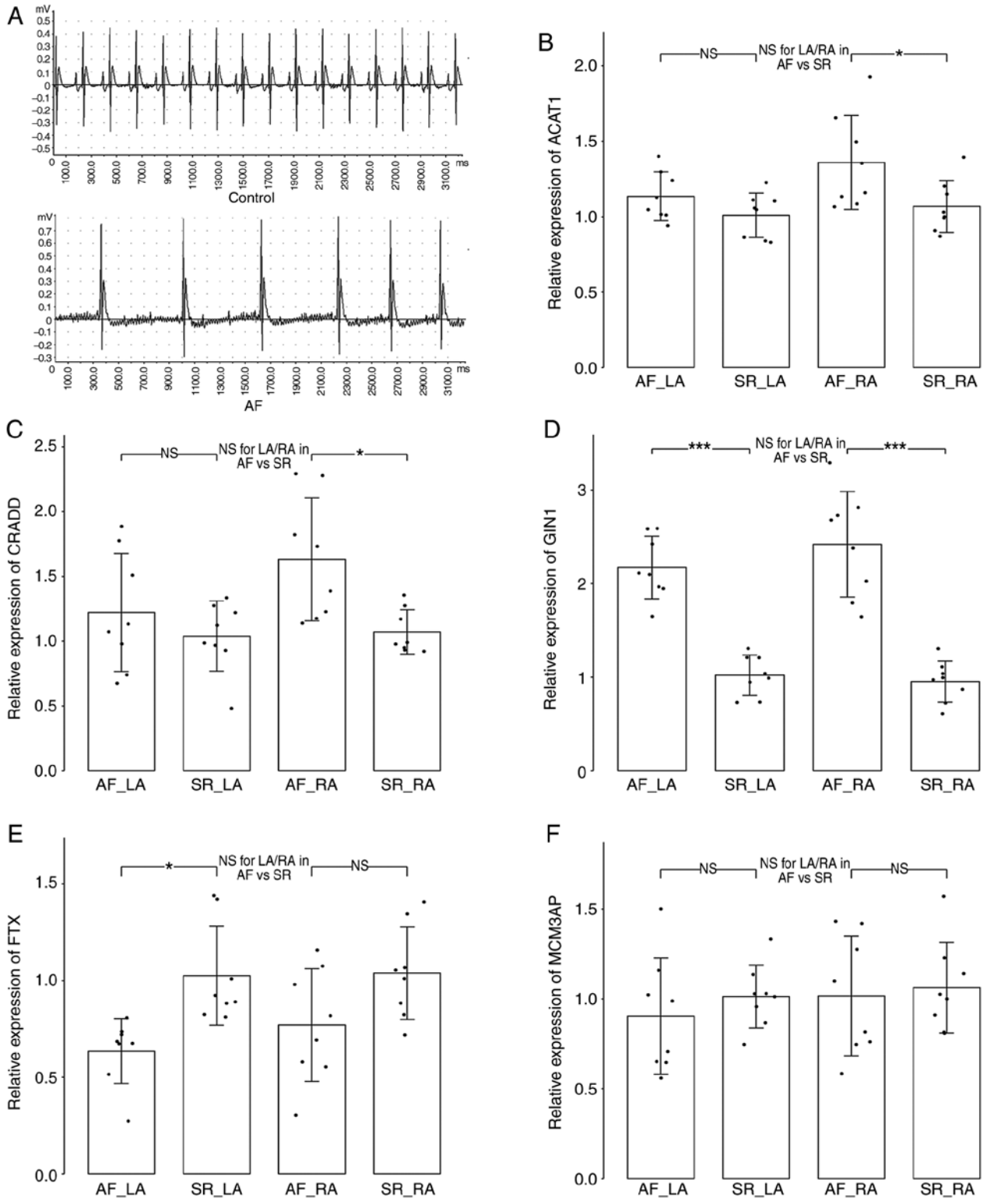

Figure 8. Validation of hub genes in AF rat models. (A) The electrocardiogram manifestations of rats in control group (SR; upper panel) and AF group (induced AF; lower panel). Validation of the expression levels of hub genes (B) ACAT1, (C) CRADD, (D) GIN1, (E) FTX and (F) MCM3AP by reverse transcription quantitative polymerase chain reaction. The relative expression levels were presented with mean ± standard deviation. *P<0.05, **P<0.01 and ***P<0.001. AF, atrial fibrillation; LA, left atria; SR, sinus rhythm; RA, right atria; ns, no statistical difference; ACAT1, acetyl-CoA Acetyltransferase 1; CRADD, death domain-containing protein CRADD; GIN1, gypsy retrotransposon integrase 1; FTX, FTX transcript, XIST regulator; MCM3AP, minichromosome maintenance complex component 3 associated protein.

cells, thereby serving an important role in early atherosclerotic lesions (47,48). Although, to the best of our knowledge, there are no studies providing evidence of a relationship between ACAT1 and AF, a close association between AF and atherosclerosis has been described (49). Therefore, ACAT1 may be associated with an increased risk of atherosclerosis in patients with AF. CRADD was demonstrated to serve a role in the regulation of apoptosis in a number of different types of tissues (50). Therefore, it may

be possible that CRADD modulates apoptosis in AF, although to date this has not been conclusively demonstrated. FTX is a lncRNA that regulates cardiomyocyte apoptosis by targeting miR-29b-1-5p and Bcl2l2 (51), therefore, it may also mediate apoptosis in AF as well. In addition, several hub genes in the magenta module were all associated with apoptosis. Apoptosis in cardiomyocytes is accompanied by fibroblast recruitment and ECM deposition in AF (52), which contributes to atrial remodeling. The data from these studies support the results of the present study that suggest the involvement of apoptosis in the pathophysiology of AF. MCM3AP is a potent natural inhibitor of initiation of DNA replication (53). TCEAL2 is a member of transcription elongation factor A (SII)-like gene family of proteins, which modulates transcription in a promoter context-dependent manner and is considered an important nuclear target for intracellular signal transduction (54). GIN1 is ubiquitously expressed in various different types of tissues, and may therefore possess an essential function (55), although the exact function remains to be determined. To the best of our knowledge, MCM3AP, TCEAL2 and GIN1 have not been studied in cardiac pathophysiology. Nevertheless, they may serve an important role in AF, as they were identified to be crucial in the AF-associated co-expression key modules and were differentially expressed between AF and SR in both atria in the present study. Therefore, future studies on the function of these hub genes in AF is required. In addition to these hub genes, a number of other genes in the green and magenta modules were also associated with pathophysiological processes of AF. For example, heat shock protein B3 and stress-70 protein, mitochondrial, present in the green module, have been demonstrated to be associated with AF (56,57), and platelet basic protein in the magenta module was associated with platelet activity and is a marker of thrombogenesis and platelet activation in AF (58).

The LA is more likely to be a driver in AF and is more likely to be associated with stroke compared with RA (15-17). The blue module was selected as another module of interest that was significantly correlated with both AF and the LA. The majority of the downregulated DADEGs were overlapped with the genes of the blue module, primarily due to the downregulated expression of LADEGs, suggesting that the genes of the blue module may be an important regulatory module of AF with an increased specificity in the LA. Enrichment analysis indicated that the blue module was primarily associated with complement, coagulation activity and ECM formation. AF is associated with elevated levels of inflammation, which contributes to thrombo-embolic complications (35,59). However, different studies have described contrasting results regarding the effects of the complement system in AF (60). A recent proteomics study demonstrated that left atrial low voltage areas (LVA) in patients with AF, which corresponded to areas of fibrotic and electrically silent myocardial tissue, were associated with an imbalance in coagulation and complement pathways, and complement and coagulation molecules were differentially expressed, including downregulation of C1q-B, C1q-C, CFH and plasminogen compared with patients without LVA (61). ECM dysregulation caused atrial fibrotic remodeling in AF through inflammation and oxidative stress (62), and studies have identified that ECM-associated genes are differentially expressed, with notable differences in gene expression between LA and RA in AF (14,63). The homeostasis between ECM composition and complement cascade effectors modulates the net effect of ECM macromolecules on the complement cascade (64). Therefore, the results of the present study suggest a complex interaction network of the complement, coagulation and ECM systems. Furthermore, the blue module was positively associated with the LA, suggesting that the blue module may be associated with the differences in hypercoagulation and structure remodeling in the different atria. Based on the results of the present and previous studies, the genes of the blue module may serve an important role in inflammation, coagulation and fibrosis, particularly in the LA, which may contribute to the pathogenesis or maladaptation of AF.

The present study has certain limitations. First, as the original article of the dataset discussed, there were no healthy controls and multiple factors including other underlying clinical traits that were not described in the dataset (14), which may have affected the reliability of the results of the present study. The analysis was focused on only 1 dataset due to the limited access to gene expression data that were collected from the paired LA and RA in patients with AF or SR. Therefore, additional datasets should be analyzed, if available, to obtain more representative results. Additionally, the pathophysiology of AF in humans is complex, and animal models could only partially reproduce the pathophysiologic spectrum of clinical AF. Further studies are required to validate these data.

In summary, WGCNA was performed on an AF dataset. Among the 20 modules, the green and magenta modules were identified as the most critical modules for AF, from which 6 hub genes, ACAT1, CRADD, GIN1, FTX, TCEAL2 and MCM3AP, were screened out, and postulated to serve key roles in pathophysiological mechanisms of AF. The green module was identified to be associated with energy metabolism, and the magenta module was associated with multiple complex interactive pathways of apoptosis and inflammation. In addition, the blue module was identified to be an important regulatory module of AF with higher specificity for the LA, and was primarily associated with complement, coagulation and ECM. These data may promote future experimental studies investigating the roles of the genes in cardiac function and pathophysiology, a number of which have not been previously described. Additionally, the genes identified may serve as novel therapeutic targets for treating patients, and assist in attaining an improved understanding of the underlying mechanisms of AF.

Acknowledgements

Not applicable.

Funding

This study was supported by the National Natural Science Foundation of China (grant nos. 91639301 and 81770458), the Key Project of Research and Development Plan of Shaanxi Province (grant no. 2017ZDCXL-SF-02-04-01), the Clinical Research Award of the First Affiliated Hospital of Xi'an Jiaotong University (grant no. XJTU1AF-CRF-2016-004), and the Natural Science Foundation of Shaanxi Province (grant no. 2018JM7063).

Availability of data and materials

The main dataset analyzed during the present study is available from the Gene Expression Omnibus repository (https://www.ncbi.nlm.nih.gov/geo) with GSE accession no., GSE79768. The DOI of the original article which generated this dataset is 10.1016/j.ijcard.2016.07.103. The two external datasets for validation are also available from GEO with GSE accession nos., GSE2240 and GSE115574.

Authors' contributions

WL performed the weighted gene co-expression network analysis and was a major contributor in writing the manuscript. LW and YW annotated the results of the network analysis and made important modifications to the manuscript. ZY and JZ designed the research project and created the final revision of the manuscript. WL and JZ performed the animal experiments in this study. All authors read and approved the final version of the manuscript.

Ethics approval and consent to participate

The animal study was approved by the Institutional Ethics Committee for Animal Experiments of Xi'an Jiaotong University. All procedures conformed to the Guide for the Care and Use of Laboratory Animals published by the National Institutes of Health.

Patient consent for publication

Not applicable.

Competing interests

The authors declare that they have no competing interests.

References

1. Zimetbaum P: Atrial Fibrillation. Ann Intern Med 166: ITC33-ITC48, 2017.
2. Odutayo A, Wong CX, Hsiao AJ, Hopewell S, Altman DG and Emdin CA: Atrial fibrillation and risks of cardiovascular disease, renal disease, and death: Systematic review and meta-analysis. BMJ 354: i4482, 2016.
3. Ferrari R, Bertini M, Blomstrom-Lundqvist C, Dobrev D, Kirchhof P, Pappone C, Ravens U, Tamargo J, Tavazzi L and Vicedomini GG: An update on atrial fibrillation in 2014: From pathophysiology to treatment. Int J Cardiol 203: 22-29, 2016.
4. Liu Y, Shi Q, Ma Y and Liu Q: The role of immune cells in atrial fibrillation. J Mol Cell Cardiol 123: 198-208, 2018.
5. Nattel S: Molecular and cellular mechanisms of atrial fibrosis in atrial fibrillation. JACC Clin Electrophysiol 3: 425-435, 2017.
6. Qian C, Li H, Chang D, Wei B and Wang Y: Identification of functional lncRNAs in atrial fibrillation by integrative analysis of the lncRNA-mRNA network based on competing endogenous RNAs hypothesis. J Cell Physiol 234: 11620-11630, 2019.
7. Prystowsky EN, Padanilam BJ and Fogel RI: Treatment of atrial fibrillation. JAMA 314: 278-288, 2015.
8. Zhang B and Horvath S: A general framework for weighted gene co-expression network analysis. Stat Appl Genet Mol Biol 4: Article17, 2005.
9. Liu S, Wang Z, Chen D, Zhang B, Tian RR, Wu J, Zhang Y, Xu K, Yang LM, Cheng C, *et al*: Annotation and cluster analysis of spatiotemporal- and sex-related lncRNA expression in rhesus macaque brain. Genome Res 27: 1608-1620, 2017.
10. Yin L, Cai Z, Zhu B and Xu C: Identification of key pathways and genes in the dynamic progression of HCC based on WGCNA. Genes (Basel) 9: E92, 2018.
11. Zhang X, Feng H, Li Z, Li D, Liu S, Huang H and Li M: Application of weighted gene co-expression network analysis to identify key modules and hub genes in oral squamous cell carcinoma tumorigenesis. OncoTargets Ther 11: 6001-6021, 2018.
12. Ahmed M, Lai TH, Zada S, Hwang JS, Pham TM, Yun M and Kim DR: Functional linkage of RKIP to the epithelial to mesenchymal transition and autophagy during the development of prostate cancer. Cancers (Basel) 10: E273, 2018.
13. Radulescu E, Jaffe AE, Straub RE, Chen Q, Shin JH, Hyde TM, Kleinman JE and Weinberger DR: Identification and prioritization of gene sets associated with schizophrenia risk by co-expression network analysis in human brain. Mol Psychiatry: Nov 26, 2018 (Epub ahead of print).
14. Tsai FC, Lin YC, Chang SH, Chang GJ, Hsu YJ, Lin YM, Lee YS, Wang CL and Yeh YH: Differential left-to-right atria gene expression ratio in human sinus rhythm and atrial fibrillation: Implications for arrhythmogenesis and thrombogenesis. Int J Cardiol 222: 104-112, 2016.
15. Gaborit N, Steenman M, Lamirault G, Le Meur N, Le Bouter S, Lande G, Léger J, Charpentier F, Christ T, Dobrev D, *et al*: Human atrial ion channel and transporter subunit gene-expression remodeling associated with valvular heart disease and atrial fibrillation. Circulation 112: 471-481, 2005.
16. Kamel H, Okin PM, Elkind MS and Iadecola C: Atrial fibrillation and mechanisms of stroke: Time for a new model. Stroke 47: 895-900, 2016.
17. Voigt N, Trausch A, Knaut M, Matschke K, Varró A, Van Wagoner DR, Nattel S, Ravens U and Dobrev D: Left-to-right atrial inward rectifier potassium current gradients in patients with paroxysmal versus chronic atrial fibrillation. Circ Arrhythm Electrophysiol 3: 472-480, 2010.
18. Liao Q, Liu C, Yuan X, Kang S, Miao R, Xiao H, Zhao G, Luo H, Bu D, Zhao H, *et al*: Large-scale prediction of long non-coding RNA functions in a coding-non-coding gene co-expression network. Nucleic Acids Res 39: 3864-3878, 2011.
19. Du Z, Fei T, Verhaak RG, Su Z, Zhang Y, Brown M, Chen Y and Liu XS: Integrative genomic analyses reveal clinically relevant long noncoding RNAs in human cancer. Nat Struct Mol Biol 20: 908-913, 2013.
20. Zhang G, Sun H, Zhang Y, Zhao H, Fan W, Li J, Lv Y, Song Q, Li J, Zhang M and Shi H: Characterization of dysregulated lncRNA-mRNA network based on ceRNA hypothesis to reveal the occurrence and recurrence of myocardial infarction. Cell Death Discov 4: 35, 2018.
21. Liao Y, Smyth GK and Shi W: The Subread aligner: Fast, accurate and scalable read mapping by seed-and-vote. Nucleic Acids Res 41: e108, 2013.
22. Langfelder P and Horvath S: WGCNA: An R package for weighted correlation network analysis. BMC Bioinformatics 9: 559, 2008.
23. Yu G, Wang LG, Han Y and He QY: clusterProfiler: An R package for comparing biological themes among gene clusters. OMICS 16: 284-287, 2012.
24. Ashburner M, Ball CA, Blake JA, Botstein D, Butler H, Cherry JM, Davis AP, Dolinski K, Dwight SS, Eppig JT, *et al*: Gene ontology: Tool for the unification of biology. The Gene Ontology Consortium. Nat Genet 25: 25-29, 2000.
25. The Gene Ontology Consortium: The Gene Ontology Resource: 20 years and still GOing strong. Nucleic Acids Res 47: D330-D338, 2019.
26. Kanehisa M and Goto S: KEGG: Kyoto encyclopedia of genes and genomes. Nucleic Acids Res 28: 27-30, 2000.
27. Kanehisa M, Sato Y, Furumichi M, Morishima K and Tanabe M: New approach for understanding genome variations in KEGG. Nucleic Acids Res 47: D590-D595, 2019.
28. Kanehisa M: Toward understanding the origin and evolution of cellular organisms. Protein Sci 28: 1947-1951, 2019.
29. Shannon P, Markiel A, Ozier O, Baliga NS, Wang JT, Ramage D, Amin N, Schwikowski B and Ideker T: Cytoscape: A software environment for integrated models of biomolecular interaction networks. Genome Res 13: 2498-2504, 2003.
30. Horvath S and Dong J: Geometric interpretation of gene coexpression network analysis. PLoS Comput Biol 4: e1000117, 2008.
31. Phipson B, Lee S, Majewski IJ, Alexander WS and Smyth GK: Robust hyperparameter estimation protects against hypervariable genes and improves power to detect differential expression. Ann Appl Stat 10: 946-963, 2016.

32. Ritchie ME, Phipson B, Wu D, Hu Y, Law CW, Shi W and Smyth GK: limma powers differential expression analyses for RNA-sequencing and microarray studies. Nucleic Acids Res 43: e47, 2015.
33. Lv X, Li J, Hu Y, Wang S, Yang C, Li C and Zhong G: Overexpression of miR-27b-3p targeting Wnt3a regulates the signaling pathway of Wnt/β-catenin and attenuates atrial fibrosis in rats with atrial fibrillation. Oxid Med Cell Longev 2019: 5703764, 2019.
34. Livak KJ and Schmittgen TD: Analysis of relative gene expression data using real-time quantitative PCR and the 2(-Delta Delta C(T)) method. Methods 25: 402-408, 2001.
35. Hu YF, Chen YJ, Lin YJ and Chen SA: Inflammation and the pathogenesis of atrial fibrillation. Nat Rev Cardiol 12: 230-243, 2015.
36. Ghezelbash S, Molina CE and Dobrev D: Altered atrial metabolism: An underappreciated contributor to the initiation and progression of atrial fibrillation. J Am Heart Assoc 4: e001808, 2015.
37. Lenski M, Schleider G, Kohlhaas M, Adrian L, Adam O, Tian Q, Kaestner L, Lipp P, Lehrke M, Maack C, *et al*: Arrhythmia causes lipid accumulation and reduced glucose uptake. Basic Res Cardiol 110: 40, 2015.
38. Heijman J and Dobrev D: Irregular rhythm and atrial metabolism are key for the evolution of proarrhythmic atrial remodeling in atrial fibrillation. Basic Res Cardiol 110: 41, 2015.
39. Mayr M, Yusuf S, Weir G, Chung YL, Mayr U, Yin X, Ladroue C, Madhu B, Roberts N, De Souza A, *et al*: Combined metabolomic and proteomic analysis of human atrial fibrillation. J Am Coll Cardiol 51: 585-594, 2008.
40. Chiang DY, Zhang M, Voigt N, Alsina KM, Jakob H, Martin JF, Dobrev D, Wehrens XH and Li N: Identification of microRNA-mRNA dysregulations in paroxysmal atrial fibrillation. Int J Cardiol 184: 190-197, 2015.
41. Harada M, Melka J, Sobue Y and Nattel S: Metabolic considerations in atrial fibrillation-mechanistic insights and therapeutic opportunities. Circ J 81: 1749-1757, 2017.
42. Zhou Q, Li L, Zhao B and Guan KL: The hippo pathway in heart development, regeneration, and diseases. Circ Res 116: 1431-1447, 2015.
43. Ikeda S and Sadoshima J: Regulation of myocardial cell growth and death by the hippo pathway. Circ J 80: 1511-1519, 2016.
44. Wang J, Liu S, Heallen T and Martin JF: The Hippo pathway in the heart: Pivotal roles in development, disease, and regeneration. Nat Rev Cardiol 15: 672-684, 2018.
45. Del Re DP, Yang Y, Nakano N, Cho J, Zhai P, Yamamoto T, Zhang N, Yabuta N, Nojima H, Pan D and Sadoshima J: Yes-associated protein isoform 1 (Yap1) promotes cardiomyocyte survival and growth to protect against myocardial ischemic injury. J Biol Chem 288: 3977-3988, 2013.
46. Leach JP, Heallen T, Zhang M, Rahmani M, Morikawa Y, Hill MC, Segura A, Willerson JT and Martin JF: Hippo pathway deficiency reverses systolic heart failure after infarction. Nature 550: 260-264, 2017.
47. Rudel LL, Lee RG and Parini P: ACAT2 is a target for treatment of coronary heart disease associated with hypercholesterolemia. Arterioscler Thromb Vasc Biol 25: 1112-1118, 2005.
48. Fazio S, Dove DE and Linton MF: ACAT inhibition: Bad for macrophages, good for smooth muscle cells? Arterioscler Thromb Vasc Biol 25: 7-9, 2005.
49. da Silva RM: Influence of inflammation and atherosclerosis in atrial fibrillation. Curr Atheroscler Rep 19: 2, 2017.
50. Ahmad M, Srinivasula SM, Wang L, Talanian RV, Litwack G, Fernandes-Alnemri T and Alnemri ES: CRADD, a novel human apoptotic adaptor molecule for caspase-2, and FasL/tumor necrosis factor receptor-interacting protein RIP. Cancer Res 57: 615-619, 1997.
51. Long B, Li N, Xu XX, Li XX, Xu XJ, Guo D, Zhang D, Wu ZH and Zhang SY: Long noncoding RNA FTX regulates cardiomyocyte apoptosis by targeting miR-29b-1-5p and Bcl2l2. Biochem Biophys Res Commun 495: 312-318, 2018.
52. Harada M, Van Wagoner DR and Nattel S: Role of inflammation in atrial fibrillation pathophysiology and management. Circ J 79: 495-502, 2015.
53. Takei Y, Assenberg M, Tsujimoto G and Laskey R: The MCM3 acetylase MCM3AP inhibits initiation, but not elongation, of DNA replication via interaction with MCM3. J Biol Chem 277: 43121-43125, 2002.
54. Kim YS, Hwan JD, Bae S, Bae DH and Shick WA: Identification of differentially expressed genes using an annealing control primer system in stage III serous ovarian carcinoma. BMC Cancer 10: 576, 2010.
55. Lloréns C and Marín I: A mammalian gene evolved from the integrase domain of an LTR retrotransposon. Mol Biol Evol 18: 1597-1600, 2001.
56. Kirmanoglou K, Hannekum A, Schafler AE: Expression of mortalin in patients with chronic atrial fibrillation. Basic Res Cardiol 99: 404-408, 2004.
57. García A, Eiras S, Parguiña AF, Alonso J, Rosa I, Salgado-Somoza A, Rico TY, Teijeira-Fernández E, González-Juanatey JR: High-resolution two-dimensional gel electrophoresis analysis of atrial tissue proteome reveals down-regulation of fibulin-1 in atrial fibrillation. Int J Cardiol 150: 283-290, 2011.
58. Lip GY, Lip PL, Zarifis J, Watson RD, Bareford D, Lowe GD and Beevers DG: Fibrin D-dimer and beta-thromboglobulin as markers of thrombogenesis and platelet activation in atrial fibrillation. Effects of introducing ultra-low-dose warfarin and aspirin. Circulation 94: 425-431, 1996.
59. Hijazi Z, Oldgren J, Siegbahn A, Granger CB and Wallentin L: Biomarkers in atrial fibrillation: A clinical review. Eur Heart J 34: 1475-1480, 2013.
60. Lappegård KT, Garred P, Jonasson L, Espevik T, Aukrust P, Yndestad A, Mollnes TE and Hovland A: A vital role for complement in heart disease. Mol Immunol 61: 126-134, 2014.
61. Kornej J, Büttner P, Hammer E, Engelmann B, Dinov B, Sommer P, Husser D, Hindricks G, Völker U and Bollmann A: Circulating proteomic patterns in AF related left atrial remodeling indicate involvement of coagulation and complement cascade. PLoS One 13: e0198461, 2018.
62. Lin CS and Pan CH: Regulatory mechanisms of atrial fibrotic remodeling in atrial fibrillation. Cell Mol Life Sci 65: 1489-1508, 2008.
63. Zhu H, Zhang W, Zhong M, Zhang G and Zhang Y: Differential gene expression during atrial structural remodeling in human left and right atrial appendages in atrial fibrillation. Acta Biochim Biophys Sin (Shanghai) 43: 535-541, 2011.
64. Gialeli C, Gungor B and Blom AM: Novel potential inhibitors of complement system and their roles in complement regulation and beyond. Mol Immunol 102: 73-83, 2018.